

Supporting Information (SI) Appendix:

SI Text

Detailed Methods:

Nanoimprinting. 50% Poly (ethylene Glycol) Di-acrylate (Mw: 200 Da), 0.1% w/v final concentration of 2-hydroxyl-1-[4-(hydroxyl) phenyl]-2-methyl-1propanone (I2959, Ciba) as photoinitiator and 5% Fluorescein Acrylate was dissolved in DMSO. A diluted 2% w/v Poly (acrylic acid) (PAA) solution was prepared in water. About 5mL of this PAA solution was spin coated on an 8” Silicon wafer at 4500 rpm for 40 seconds. The wafer was then baked on a hot plate at 160°C for 1 minute. Nanoimprinting was carried out using the Jet and Flash Imprint Lithography (J-FIL™) process on an Imprio® 100, Molecular Imprints Inc., Austin, TX. For details of the J-FIL™ based imprinting process see SI Appendix.

J-FIL™ based nanoimprinting: In the J-FIL™ process, a pre-patterned transparent quartz template was pressed onto resist droplets which were inkjetted onto a silicon wafer pre-coated with PAA release layer, causing it to spread, and fill the features in the quartz mold. The resist was then exposed to UV light (365nm wavelength at 5 mW/cm² intensity), for 25 seconds to photopolymerize the molded resist. The template was then demolded, revealing the desired nanostructures. The imprints were sputter coated with 3nm layer of Platinum and the residual layer was measured using cross-sectional SEM. A low power (35 Watts) Argon plasma etch (Oxford Instruments Plasma Lab 80+) was performed at a pressure of 10 mTorr with Ar (20 sccm) and O₂ (4 sccm) yielding an etch rate of 0.6nm/sec.

Release and Characterization of Nanoparticles. Imprints were washed twice with DMSO after etching on the wafer to remove any unreacted polymer. Imprints were then submerged in DMSO, incubated for 5 minutes and blow dried with Nitrogen. Nanoparticles were harvested by pipetting

50 μ l of filtered de-ionized (DI) water over a 5mmx5mm imprint area. The DI water is used to dissolve the underlying PAA layer and the DI water containing the released nanoparticles was then collected after 1 minute. The water containing nanoparticles was dialyzed for 3 days using 300KDa Float-A-Lyzer (SpectrumLabs Inc.). For SEM, 3 μ l of nanoparticle suspension was dispensed on a SEM stub, air-dried and sputter coated with 3nm layer of Platinum to make the sample conductive. For fluorescence microscopy, 3 μ l of nanoparticle suspension was dispensed on a glass slide and covered with a glass cover slip. Imaging was done at 100X magnification by exciting the sample using a 488nm wavelength laser. Zeta potential and dynamic light scattering analysis was performed using a Zetasizer nano ZS tool (Malvern Inc.). Zeta potential analysis was performed by Dr. Claudia Mujat, Malvern Inc. For serum stability tests, dialyzed nanoparticles were mixed with 10% serum containing PBS and imaged using fluorescence microscopy directly in serum containing PBS. For long term serum stability, dialyzed nanoparticles were mixed with 10% serum containing PBS or just PBS as control and incubated at 37°C for 48 hours. The solution was then dialyzed in 1000KDa float-a-lyzer (Spectrum Labs) for 2 days against deionized water.

Cell Culture. HeLa (ATCC) and HEK 293 (ATCC) cells were cultured in Dulbecco's Modified Eagle Medium (DMEM) (Hyclone) supplemented with 10% fetal bovine serum (Characterized FBS, Hyclone) and 1% antibiotics (penicillin and streptomycin, Invitrogen). HUVEC (ATCC) cells were cultured in MCDB 131 medium (Life Technologies) supplemented with 10% fetal bovine serum (Characterized FBS, Hyclone) and 1% antibiotics (penicillin and streptomycin, Invitrogen) and further supplemented with EGM2 Supplement and growth factor kit (Lonza Inc.). mCherry labeled clathrin cell lines of RPE cells (gift from Dr. Marcel Mettlen at UT Southwestern Medical Center, Dallas) were cultured in DMEM/Ham's F12 1:1 mixture

supplemented with 10% fetal bovine serum (Characterized FBS, Hyclone) and 1% antibiotics (penicillin and streptomycin, Invitrogen). Similar green fluorescent protein (GFP) labeled clathrin cell lines have been previously reported (1). Mouse lung microvasculature endothelial cells were isolated as previously described (2) and cultured in MCDB 131 medium supplemented with 5% fetal bovine serum and 1% antibiotics. For all cell lines, media was changed every other day and cells were passaged at 80-90% confluency. Bone Marrow Dendritic Cells (BMDCs) were derived from bone marrow isolated progenitor cells of female Balb/c mice (H-2d, 5-10 weeks old, Jackson Laboratories). RPMI-1640 Glutamax® (Invitrogen, Carlsbad, CA) medium, supplemented with 20 ng/ml mouse GM-CSF and 10 ng/ml IL4 (eBioscience, San Diego, CA) was used to differentiate progenitor cells into the myeloid lineage. Loosely adherent APCs (a mixture of cells with mostly DCs) were harvested on day 6-7 and found to be 70-75% CD11c+. All of the experimental and surgical procedures involving animals were approved by the University of Texas at Austin Institutional Animal Care and Use Committee. BMDCs were used immediately and isolated fresh from mice for each experiment.

Cytotoxicity Assay. HeLa, HEK293 and HUVEC cells were used for *in vitro* cytotoxicity analysis of the fabricated PEGDA nanocarriers using an MTS assay (CellTiter 96 AQueous One Solution Cell Proliferation Assay, Promega). 10,000 cells were plated overnight in a 96 well plate. Assays were performed by adding the MTS reagent solution to culture wells and recording the absorbance (at 490nm) at after particle incubation of 48 hours. A ratio of 10^5 nanoparticles of 325nm x 100nm discs and 400nm x 100nm x 100nm rods per cell was used. All the experiments were done in groups of 6.

Thermo-Gravimetric Analysis. The weights of a known amount of fluorescence unit containing nanoparticles for different shapes were measured using thermo-gravimetric analysis (TGA)

(Mettler Toledo). Fluorescence intensity of 100 and 50 units of were measured on a Biotech plate reader for 3 different shapes of nanoparticles solutions using excitation filters 480/20nm and emission filters 520/20nm. The solution was then subjected to heating till 150°C for 20 mins to evaporate all solvent and dry weight was measured.

Confocal Microscopy. For Confocal Microscopy, HeLa and RPE cells were seeded (20,000 cells per well) on poly-l-lysine coated coverslips (BD BiocoatTM) in a 24 well tissue culture plate and then allowed to adhere overnight. Cells were then incubated with nanoparticles for 24 hours. Cells were then fixed, permeabilized and their nuclei stained using DAPI (Molecular Probes). HeLa cells cytoskeleton was also stained using Texas Red conjugated phalloidin (Molecular Probes). RPE cells have inherent red fluorescently labeled (mCherry) clathrin pits. Slides were imaged using a Leica SP2 AOBS confocal microscope.

Flow Cytometry. For flow cytometry, HeLa, HEK293, HUVEC and mouse lung microvasculature endothelial cells were seeded (20,000 cells per well) in a 24 well tissue culture plate and then allowed to adhere overnight in 10% serum containing medium. Cells were then incubated with equal mass of shape-specific particles or polystyrene beads for 12, 24 and 48 hours. Cells were then trypsinized, washed with phosphate buffer saline (PBS) and resuspended into 2% FACS buffer (2% FBS in PBS). Flow cytometry was done using Accuri C6 cytometer (BD AccuriTM). All conditions were done in triplicates. For BMDCs, 100,000 cells per well were seeded in a 48 well tissue culture plate and same process was repeated. Change in median fluorescence was calculated and integer values were plotted against time. At each time point background fluorescence was measured using untreated cells at that time point and subtracted from test samples to obtain change in median fluorescence. At time $t = 0$ hours particle uptake was assumed to be zero. To compare number of particles internalized among various shapes,

80nm x 70nm disc particles were used to normalize all particles. It was assumed that change in median fluorescence for 80nm diameter disc corresponds to 100 particles per cell and the number of particles for other shapes were computed relatively using the following formula.

$$\text{Number of particles for a specific shape} = \frac{\text{Change in Median Fluorescence for that shape} \times \text{Volume of (80nm x 70nm) disc} \times 100}{\text{Volume of that Specific Shape}}$$

Inverted Culture Studies. For inverted culture studies, HEK 293 and HUVEC cells were seeded (20,000 cells per well) on poly-l-lysine coated cover slips in a 24 well tissue culture plate and then allowed to adhere overnight. Cover slips were then gently placed inverted onto 2 glass pegs of equal size (1mm cube) and media filled up to 1.3 mm in each well. Equal fluorescence of polystyrene beads and shape specific particles were then incubated with cells for 24 and 48 hours after which cover slips were transferred into a fresh 24 well plate. Cells were then trypsinized, washed with phosphate buffer saline (PBS) and resuspended into 2% FACS buffer (2% FBS in PBS) for flow cytometry. One experimental repeat was discarded as an outlier as the trend for one of the particle shape was not consistent with other 5 experimental repeats.

Pharmacological Inhibition studies. For Pharmacological inhibitors Studies, HEK293 and HUVEC cells were seeded (20,000 cells per well) in a 24 well tissue culture plate and then allowed to adhere overnight. Various pharmacological inhibitors were used and added to cells at the concentration described in **Fig 3A**. Cells were incubated for 1 hour after which particles were added to cells (25 μ g/ml) containing inhibitors for 5 more hours. Cells were then trypsinized, washed with phosphate buffer saline (PBS) and resuspended into 2% FACS buffer (2% FBS in PBS) for flow cytometry and analyzed as described above. Data shows average and standard deviation from three independent inhibition experiments.

Strain Energy Calculations. In order to calculate the curvature strain energy required for a cell membrane to wrap around a particle we began by assuming that the endosomal shape is dependent on the particle geometry. We used the Canham-Helfrich formulation to calculate the curvature energy required for the lipid bilayer to conform and envelope a particle of a given shape. **SI Appendix (Figure S13)** shows the assumed endosomal shape enveloping either the rod or disc-shaped particle. The following expression describes the curvature energy (3).

$$E_c = \oint \left[\frac{1}{2} k_c (c_1 + c_2 + 2c_s)^2 + k_s c_1 c_2 \right] dA$$

where k_c is the curvature modulus, c_1 and c_2 are the principle curvatures of the final vesicle shape, c_s is the spontaneous curvature, and k_s is the saddle-splay modulus. The product of c_1 and c_2 is known as the Gaussian curvature and can be ignored for a homogeneous lipid bilayer (4).

With this assumption, the expression reduces to

$$E_c = \oint \left[\frac{1}{2} k_c (c_1 + c_2 + 2c_s)^2 \right] dA$$

Integrating this expression over the area of the assumed endosome shape gives the curvature energy. For rod-shaped particles, the endosomal surface reduces to a single sphere of radius $\frac{c}{2}$, a cylinder of radius $\frac{c}{2}$ and length b , a second cylinder of radius $\frac{b}{2}$ and length a , and two rectangles of zero curvature. The disc-shaped particles experience a vesicle shape assumed to be the outer half of a torus with wheel radius R and tube radius p along with two circular, zero curvature, areas of πR^2 each.

For the rod-shaped particle the integral takes the following form

$$E_{c_{rod}} = \oint \frac{1}{2} k_c \left(\frac{1}{r} + 2c_s \right)^2 dA + \oint \frac{1}{2} k_c \left(\frac{2}{r} + 2c_s \right)^2 dA$$

after evaluating the integral and substituting $r = \frac{c}{2}$ the required curvature energy is

$$E_{c_{rod}} = \pi k_c \left[2c(a+b) \left(\frac{1}{c} + c_s \right)^2 + 2(2 + cc_s)^2 \right]$$

For the disc-shaped particle the curvature energy term (5) is

$$E_{c_{disc}} = \pi k_c \int_{-\frac{\pi}{2}}^{\frac{\pi}{2}} \left(\frac{R + 2p \cos(\theta)}{2p(R + p \cos(\theta))} + 2c_s \right)^2 p(R + p \cos(\theta)) d\theta$$

where $p(R + p \cos(\theta))$ is the Jacobian for the half torus for which θ is integrated from $-\frac{\pi}{2}$ to $\frac{\pi}{2}$.

This expression becomes:

$$E_{c_{disc}} = \pi k_c \left\{ 2(1 + 2pc_s)(\pi c_s R + 2pc_s + 1) + \left[\frac{R^2 \tan^{-1} \left(\sqrt{1 - \frac{2p}{p+R}} \right)}{p\sqrt{R^2 - p^2}} \right] \right\}$$

Values for k_c are typically taken to be $20K_B T$ but interestingly have been shown to be as high as $285K_B T$ for clathrin (6). The value for c_s is take to be $1/40 \text{ nm}^{-1}$ (7). **SI Appendix (Table S2)** shows the curvature energy of each endosome shape normalized by the value for the most energetically costly shape, that of the $800\text{nm} \times 100\text{nm} \times 100\text{nm}$ rod, and indicates that rods require more bending energy to envelope than discs. In comparison, the curvature energy required to envelope a sphere when the spontaneous curvature term is included has a r^2 dependence which is consistent with experimental data showing smaller spheres are more easily uptaken by cells (as shown in **SI Appendix (Fig. S5)**). The model used here is geometric and fits some of the experimental data in **Fig. 2** but does not fully describe the complex and active process of endocytosis. It does however suggest that macropinocytosis is a geometry-dependent process.

References for SI text:

1. Loerke D, Mettlen M, Schmid SL, & Danuser G (2011) Measuring the hierarchy of molecular events during clathrin-mediated endocytosis. *Traffic* 12(7):815-825.
2. Dong QG, *et al.* (1997) A general strategy for isolation of endothelial cells from murine tissues. Characterization of two endothelial cell lines from the murine lung and subcutaneous sponge implants. *Arterioscler Thromb Vasc Biol* 17(8):1599-1604.
3. Helfrich W (1973) Elastic properties of lipid bilayers: theory and possible experiments. *Z Naturforsch C* 28(11):693-703.
4. Das SL, Jenkins JT, & Baumgart T (2009) Neck geometry and shape transitions in vesicles with co-existing fluid phases: Role of Gaussian curvature stiffness vs. spontaneous curvature. *Epl-Europhys Lett* 86(4).
5. O'Neill B & Ebooks Corporation Limited. (2006) Elementary Differential Geometry. (Elsevier Science, Burlington), p 1 online resource (518 p.).
6. Jin AJ, Prasad K, Smith PD, Lafer EM, & Nossal R (2006) Measuring the elasticity of clathrin-coated vesicles via atomic force microscopy. *Biophys J* 90(9):3333-3344.
7. Leikin S, Kozlov MM, Fuller NL, & Rand RP (1996) Measured effects of diacylglycerol on structural and elastic properties of phospholipid membranes. *Biophysical journal* 71(5):2623-2632.

SI Figure legends:

Fig. S1: Particle characterization in presence of serum shows no aggregation of particles: **A)** Fluorescence Microscopy images of 220nm diameter x 100nm height particles at excitation wavelength of 488nm and emission at 520nm, **B)** SEM image of 400nm x 100nm x 100nm particles after incubation in 10% serum.

Fig. S2: *In vitro* cytotoxicity assay show particles are non-toxic. Cytotoxicity assay for HeLa, HEK 293 and HUVEC cells conducted with 325 nm x 100 nm discs and 400 nm x 100 nm x 100nm rod shaped particles. Error bars are standard deviation with n=6 for each data point

Fig. S3: Correlation of fluorescence signal with mass of nanoparticle. Plot showing correlation between fluorescence units and mass of particles.

Fig. S4: Confocal Microscopy of particle uptake by HeLa cells. Confocal cross-section images of HeLa cells showing internalization of shape-specific particles **A)** 80nm diameter x 70nm height discs, **B)** 220nm diameter x 100nm height discs, **C)** 325nm diameter x 100nm height discs, **D)** 400nm x 100nm x 100nm rods, **E)** 800nm x 100nm x 100nm rods.

Fig. S5: Flow cytometry kinetic plots for uptake of polystyrene beads in 4 cell lines. Effect of size of nanoparticles on uptake kinetics in **A)** HeLa cells, **B)** HEK 293 cells, **C)** HUVEC cells, **D)** BMDCs. In figure a-d, dashed green line for 200nm polystyrene spherical particles and solid green line for 100nm polystyrene spherical particles. Error bars are standard deviation with n=3 for each data point.

Fig S6: Cellular uptake of shape specific nanoparticles after 24 hours in Mouse Lung Endothelial Cells. Dashed red bars for 220nm x 100nm disc and dashed blue bars for 400nm x 100nm x 100nm. Error bars are standard deviation with n=3 for each data point.

Fig. S7: Cellular uptake kinetics of different shape-specific nanoparticles in various cell lines. **A)** HeLa cells, **B)** HEK 293 cells, **C)** HUVEC cells, **D)** BMDCs. In figure A-D, red lines are for nanodiscs (hollow for 325x100nm disc, dashed for 220x100nm disc and solid for 80x70nm disc) and blue lines for nanorods (dashed for 400x100x100nm rods and solid for 800x100x100nm rods). Error bars are standard deviation with n=3 for each data point.

Fig. S8: Inverted Culture Uptake studies: Inverted cellular uptake of shape specific nanoparticles after 24 hours in **A)** HEK 293 cells, **B)** HUVEC cells. Red bars are for discs (hollow red bars for 325nm x 100nm disc, dashed red bars for 220nm x 100nm disc and solid red bars for 80nm x 70nm disc) and blue bars for rods (dashed blue bars for 400nm x 100nm x 100nm and solid blue bars for 800nm x 100nm x 100nm). Error bars are standard deviation with n=3 for each data point.

Fig S9: Cellular uptake of different shape-specific nanoparticles after 6 hours of incubation with **A)** HEK 293 cells, and **B)** HUVEC cells. In this figure, red bars are for nanodiscs (hollow for 325x100nm disc, dashed for 220x100nm disc and solid for 80x70nm disc) and blue bars for nanorods (dashed for 400x100x100nm rods and solid for 800x100x100nm rods). Error bars are standard deviation with n=3 for each data point.

Fig. S10: Effect of pharmacological inhibitors on uptake of various shape-specific nanoparticles. Change in normalized median fluorescence uptake of shape specific particles due to presence of inhibitors in HeLa cells. Error bars are standard deviation with n=3 for each data point. Red bars are for nanodiscs (solid for 80nm diameter discs, dashed for 220nm diameter and hollow for 325nm diameter) and blue lines for nanorods (dashed for 400x100x100nm rods and solid for 800x100x100nm rods).

Fig. S11: Confocal Microscopy of particle uptake and localization by clathrin labeled RPE cells. Confocal Images of RPE cell lines incubated with shape-specific particles to test the co-localization of particles with clathrin pits. **A)** 80nm diameter x 70nm height discs, **B)** 220nm diameter x 100nm height discs, **C)** 325nm diameter x 100nm height discs, **D)** 400nm x 100nm x 100nm rods, **E)** 800nm x 100nm x 100nm rods.

Fig. S12: Effect of Pharmacological Inhibitors on uptake of spherical polystyrene nanoparticles. Change in normalized median fluorescence uptake due to presence of inhibitors in HEK 293 Cells. Solid green bars are for 100nm diameter polystyrene beads, dashed green bars are for 200nm diameter polystyrene beads and hollow green bars are for 500nm diameter polystyrene beads. Error bars are standard deviation with n=5 for each data point.

Fig. S13: Particle shapes (solid blue) and assumed endosome shapes during macropinocytosis (blue outline).

Table S2: Normalized values for the curvature energy required to envelope a particle with a lipid bilayer for the five particles geometries used in uptake studies. The values show that discs are more easily uptaken than rods. These theoretical results agree qualitatively with experimental results for particle uptake in epithelial cells.

SI Figures

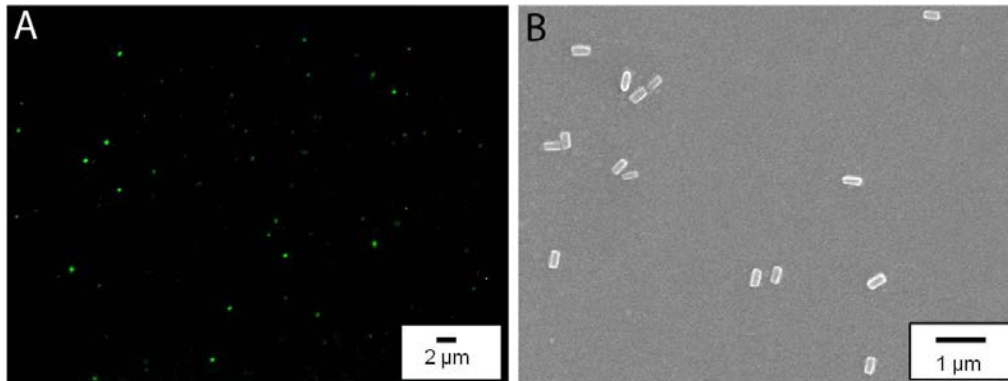


Fig. S1: Particle characterization in presence of serum shows no aggregation of particles: **A)** Fluorescence Microscopy images of 220nm diameter x 100nm height particles at excitation wavelength of 488nm and emission at 520nm, **B)** SEM image of 400nm x 100nm x 100nm particles after incubation in 10% serum.

Table S1: DLS and Zeta potential characterization of particles after incubation in 10% serum:

400x100x100nm particles	Particle in PBS	Particle in FBS
DLS	$452.2 \pm 20\text{nm}$	$458.9 \pm 16\text{nm}$
Zeta	$-55 \pm 4 \text{ mV}$	$-48 \pm 3 \text{ mV}$

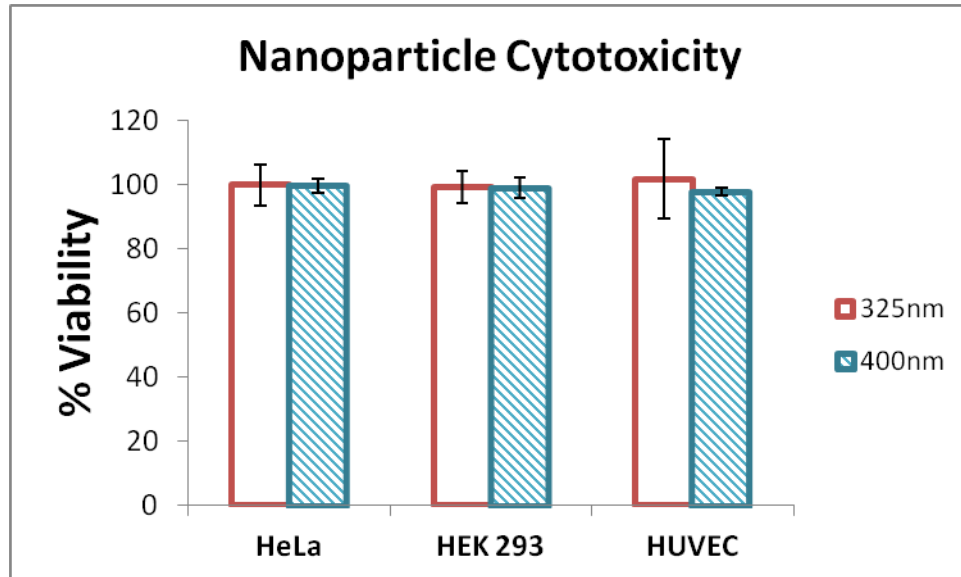


Fig. S2: *In vitro* cytotoxicity assay show particles are non-toxic. Cytotoxicity assay for HeLa, HEK 293 and HUVEC cells conducted with 325 nm x 100 nm discs and 400 nm x 100 nm x 100nm rod shaped particles. Error bars are standard deviation with n=6 for each data point

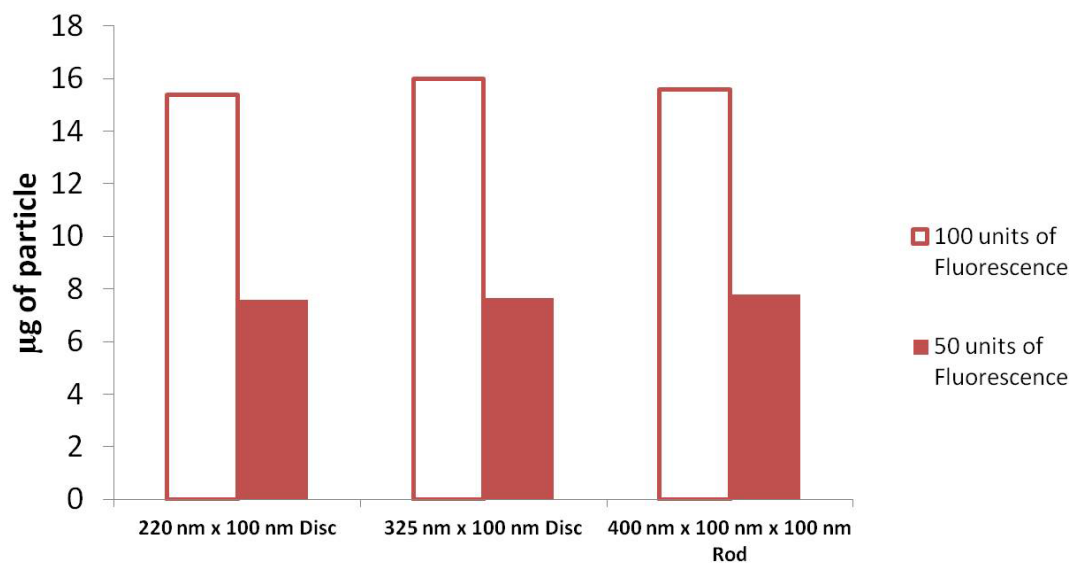


Fig. S3: Correlation of fluorescence signal with mass of nanoparticle. Plot showing correlation between fluorescence units and mass of particles.

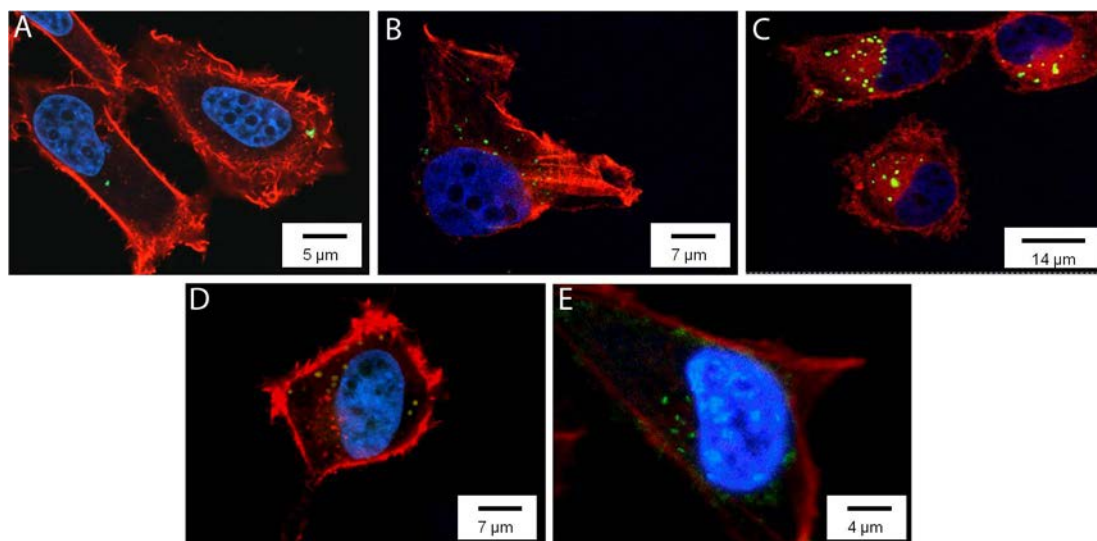


Fig. S4: Confocal Microscopy of particle uptake by HeLa cells. Confocal cross-section images of HeLa cells showing internalization of shape-specific particles **A)** 80nm diameter x 70nm height discs, **B)** 220nm diameter x 100nm height discs, **C)** 325nm diameter x 100nm height discs, **D)** 400nm x 100nm x 100nm rods, **E)** 800nm x 100nm x 100nm rods.

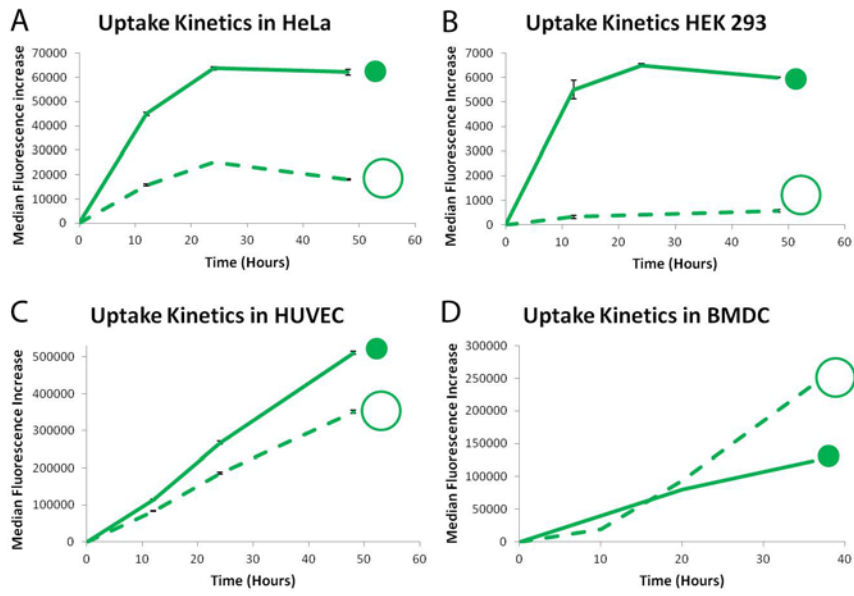


Fig. S5: Flow cytometry kinetic plots for uptake of polystyrene beads in 4 cell lines. Effect of size of nanoparticles on uptake kinetics in **A)** HeLa cells, **B)** HEK 293 cells, **C)** HUVEC cells, **D)** BMDCs. In figure a-d, dashed green line for 200nm polystyrene spherical particles and solid green line for 100nm polystyrene spherical particles. Error bars are standard deviation with n=3 for each data point.

Median Fluorescence Increase in Mouse Lung Endothelial Cells

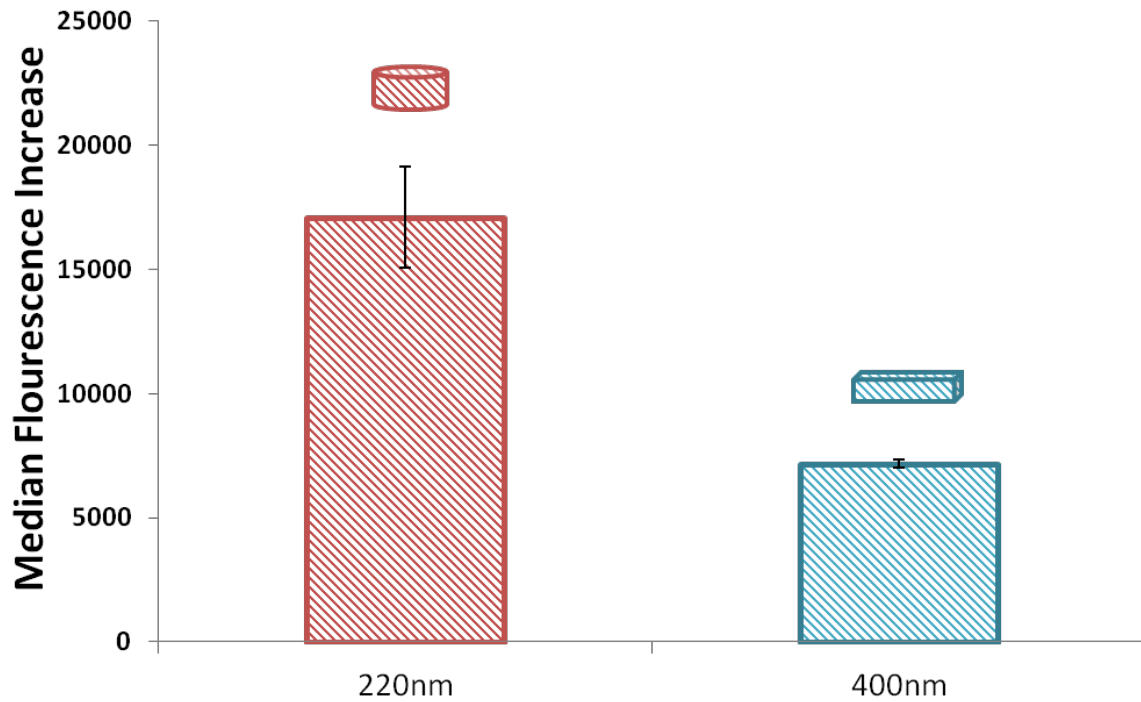


Fig S6: Cellular uptake of shape specific nanoparticles after 24 hours in Mouse Lung Endothelial Cells. Dashed red bars for 220nm x 100nm disc and dashed blue bars for 400nm x 100nm x 100nm. Error bars are standard deviation with n=3 for each data point.

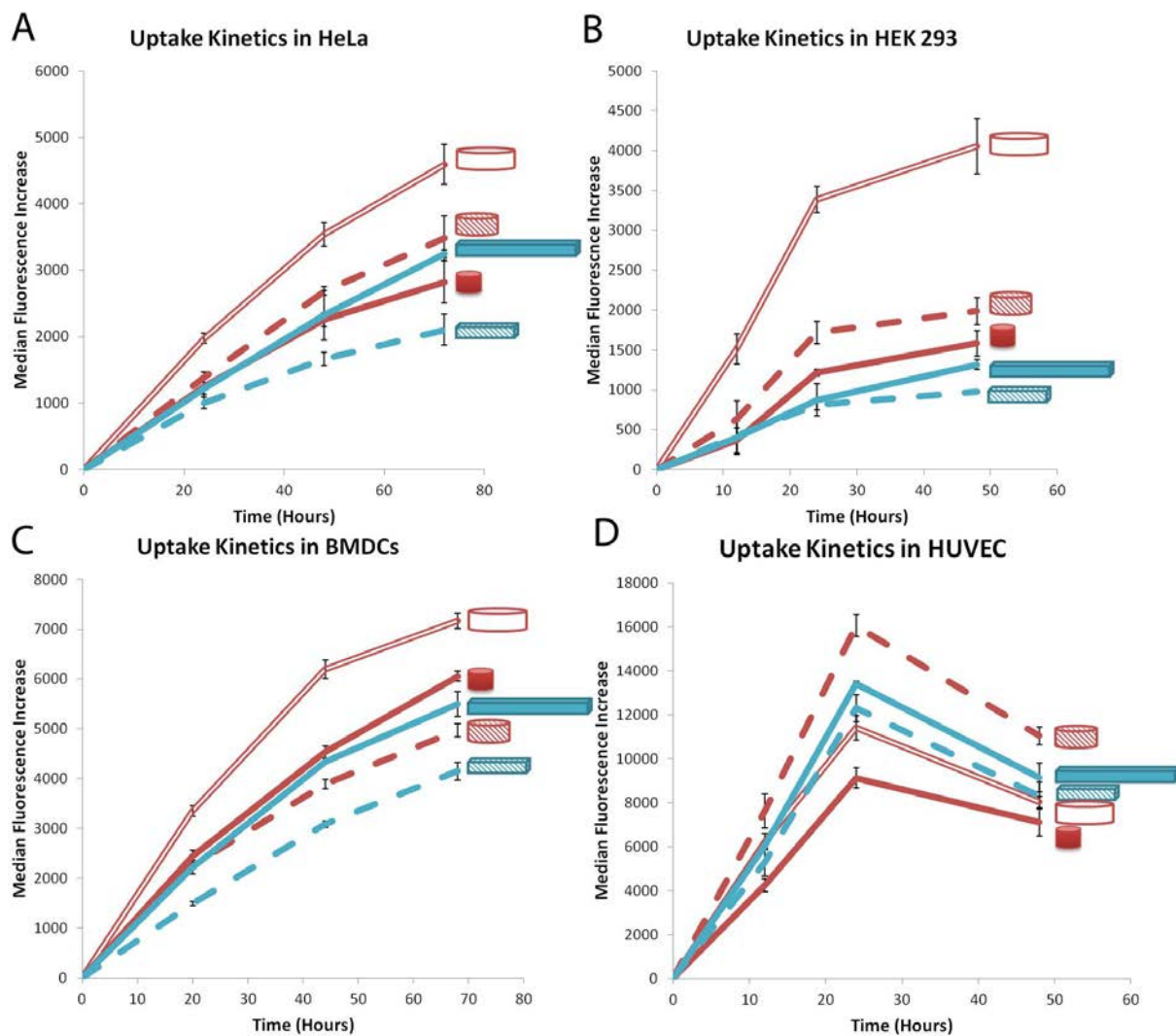


Fig. S7: Cellular uptake kinetics of different shape-specific nanoparticles in various cell lines. **A)** HeLa cells, **B)** HEK 293 cells, **C)** HUVEC cells, **D)** BMDCs. In figure A-D, red lines are for nanodiscs (hollow for 325x100nm disc, dashed for 220x100nm disc and solid for 80x70nm disc) and blue lines for nanorods (dashed for 400x100x100nm rods and solid for 800x100x100nm rods). Error bars are standard deviation with n=3 for each data point.

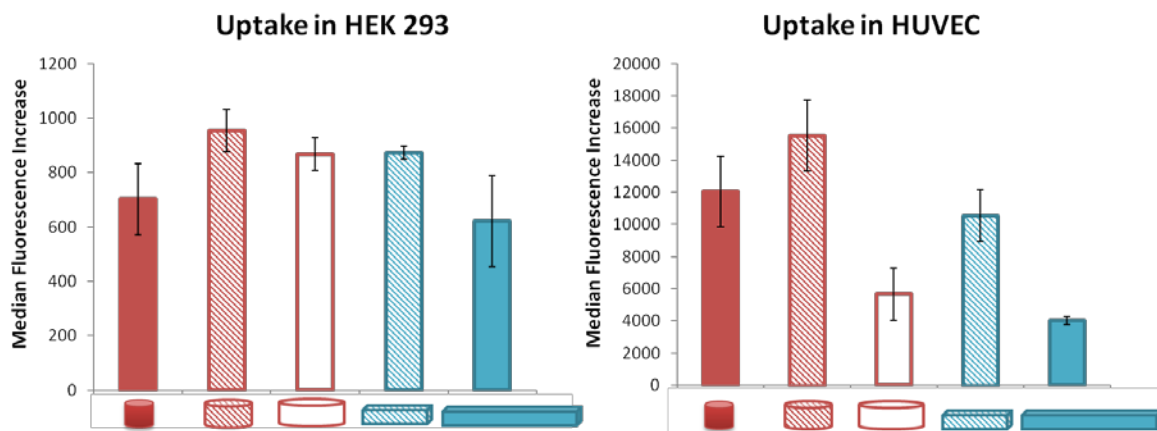


Fig. S8: Inverted Culture Uptake studies: Inverted cellular uptake of shape specific nanoparticles after 24 hours in **A)** HEK 293 cells, **B)** HUVEC cells. Red bars are for discs (hollow red bars for 325nm x 100nm disc, dashed red bars for 220nm x 100nm disc and solid red bars for 80nm x 70nm disc) and blue bars for rods (dashed blue bars for 400nm x 100nm x 100nm and solid blue bars for 800nm x 100nm x 100nm). Error bars are standard deviation with n=3 for each data point.

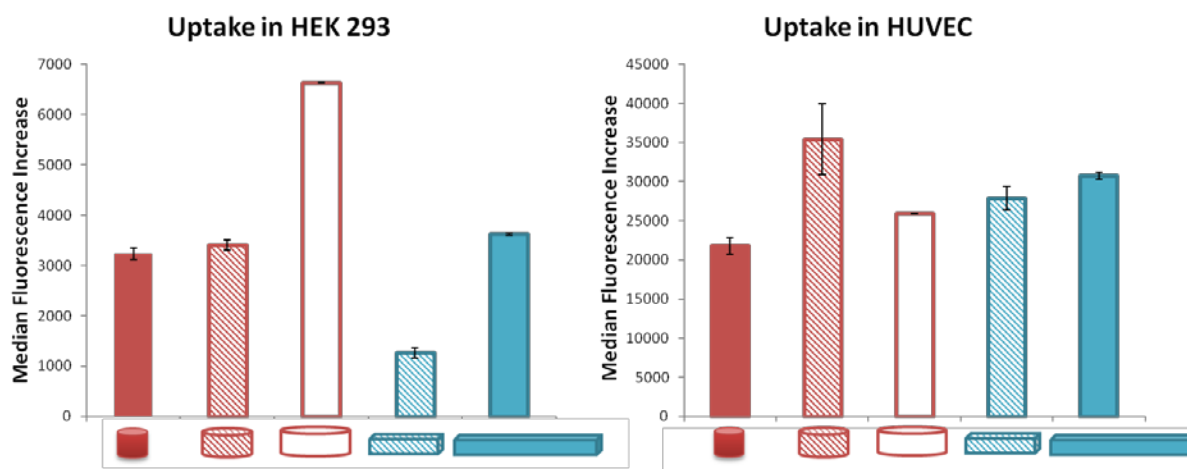


Fig S9: Cellular uptake of different shape-specific nanoparticles after 6 hours of incubation with **A)** HEK 293 cells, and **B)** HUVEC cells. In this figure, red bars are for nanodiscs (hollow for 325x100nm disc, dashed for 220x100nm disc and solid for 80x70nm disc) and blue bars for nanorods (dashed for 400x100x100nm rods and solid for 800x100x100nm rods). Error bars are standard deviation with n=3 for each data point.

Effect of inhibitors on uptake in HeLa cells

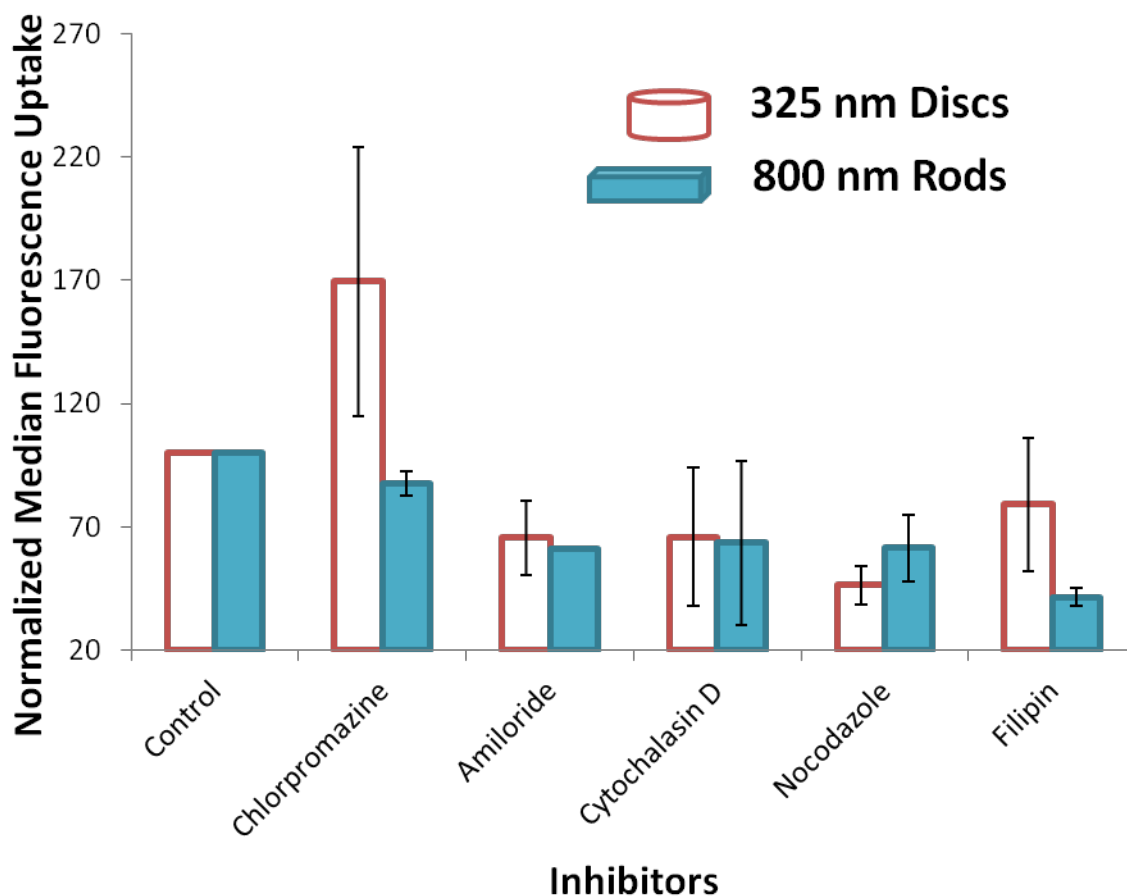


Fig. S10: Effect of pharmacological inhibitors on uptake of various shape-specific nanoparticles. Change in normalized median fluorescence uptake of shape specific particles due to presence of inhibitors in HeLa cells. Error bars are standard deviation with n=3 for each data point. Red bars are for nanodiscs (solid for 80nm diameter discs, dashed for 220nm diameter and hollow for 325nm diameter) and blue lines for nanorods (dashed for 400x100x100nm rods and solid for 800x100x100nm rods).

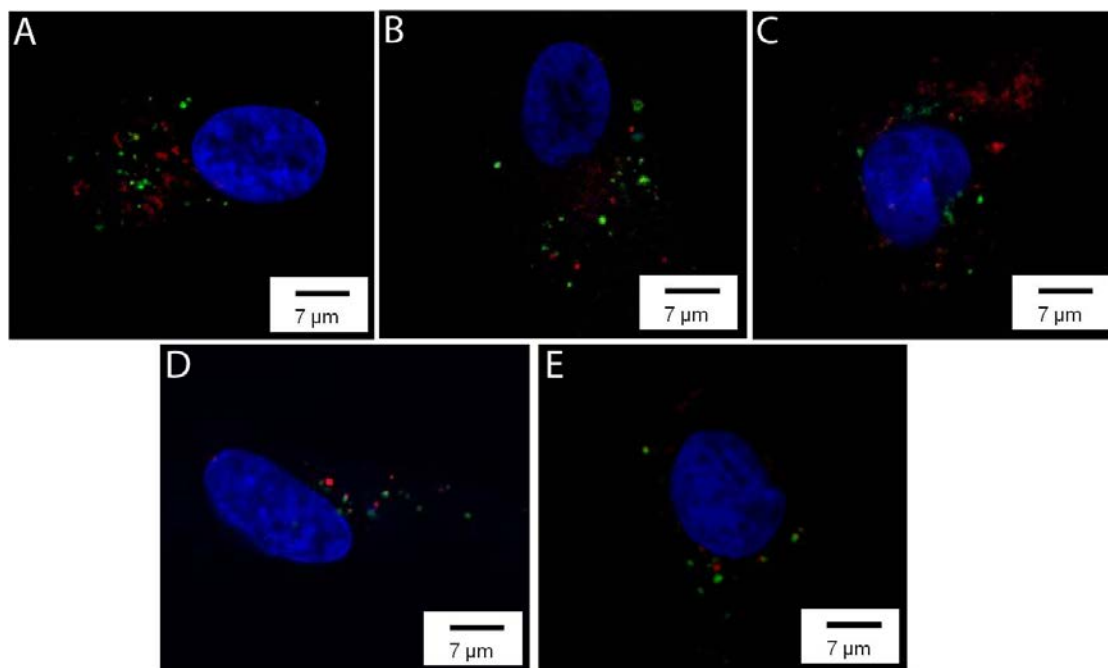


Fig. S11: Confocal Microscopy of particle uptake and localization by clathrin labeled RPE cells. Confocal Images of RPE cell lines incubated with shape-specific particles to test the co-localization of particles with clathrin pits. **A)** 80nm diameter x 70nm height discs, **B)** 220nm diameter x 100nm height discs, **C)** 325nm diameter x 100nm height discs, **D)** 400nm x 100nm x 100nm rods, **E)** 800nm x 100nm x 100nm rods.

Effect of inhibitors on uptake in HEK 293

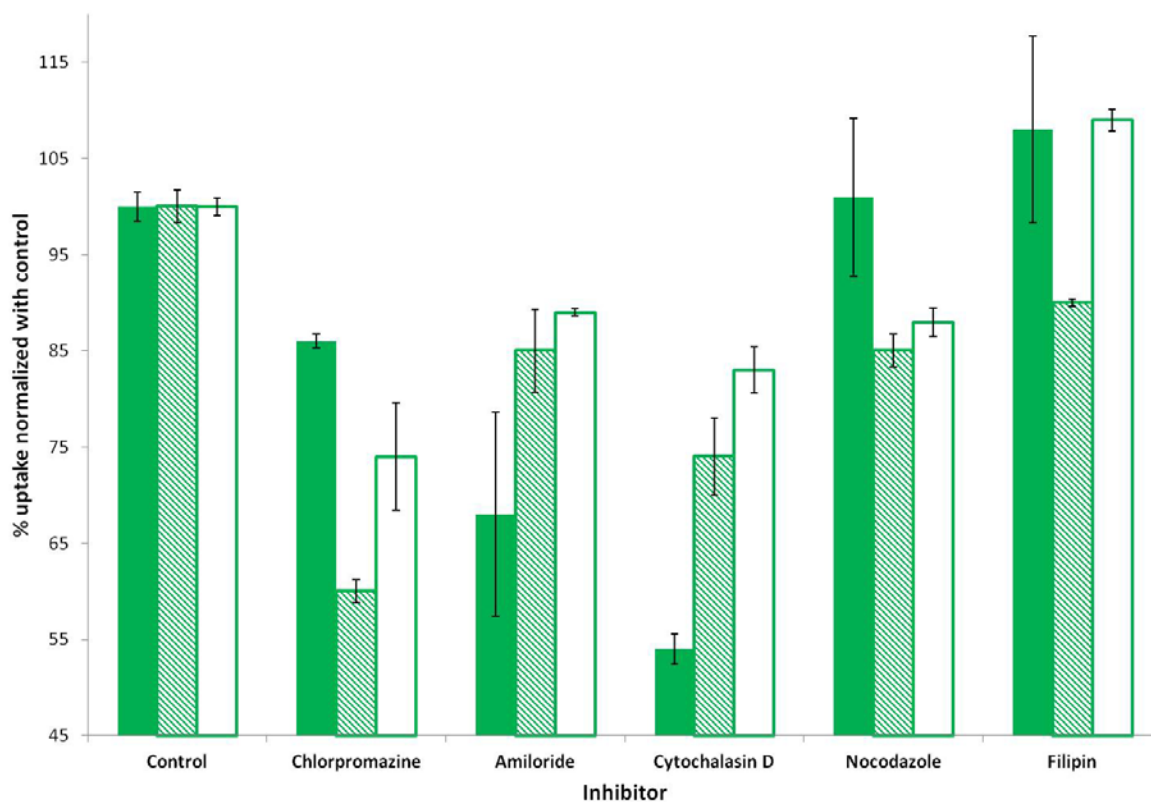


Fig. S12: Effect of Pharmacological Inhibitors on uptake of spherical polystyrene nanoparticles.

Change in normalized median fluorescence uptake due to presence of inhibitors in HEK 293

Cells. Solid green bars are for 100nm diameter polystyrene beads, dashed green bars are for

200nm diameter polystyrene beads and hollow green bars are for 500nm diameter polystyrene

beads. Error bars are standard deviation with n=5 for each data point.

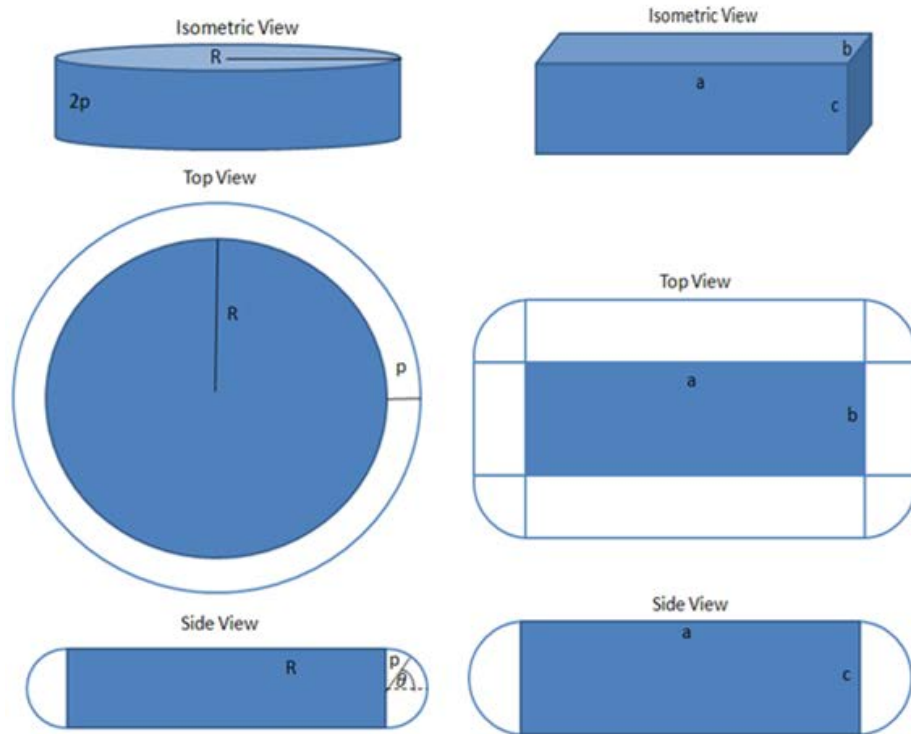


Fig. S13: Particle shapes (solid blue) and assumed endosome shapes during macropinocytosis (blue outline).






Normalized Curvature Energies	
1.000	
0.625	
0.444	
0.331	
0.126	

Table S2: Normalized values for the curvature energy required to envelope a particle with a lipid bilayer for the five particles geometries used in uptake studies. The values show that discs require less energy than rods. These theoretical results agree qualitatively with experimental results for particle uptake in epithelial cells.